#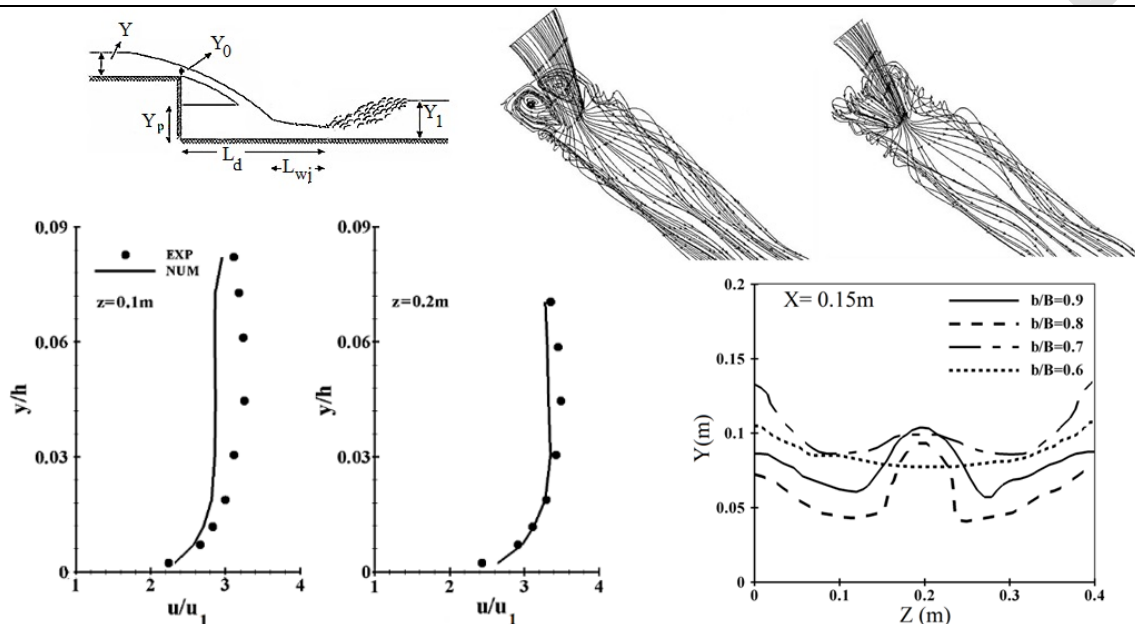 Numerical investigation of flow field characteristics over vertical drops with sudden contraction for different contraction ratios

Hossein Shahin[iD], **Afshin Eghbalzadeh*** [iD], **Mitra Javan**[iD]

Department of Civil Engineering, Faculty of Engineering, Razi University, Kermanshah, Iran.

GRAPHICAL ABSTRACT

ABSTRACT

Vertical drops are widely implemented in hydraulic structures such as irrigation canals, wastewater collection systems, and stepped spillways to dissipate flow kinetic energy while enhancing aeration and promoting dissolved oxygen levels. Depending on local topography, these structures serve to reduce the kinetic energy of falling water and to regulate the flow velocity within canals and irrigation networks. In this study, a three-dimensional numerical simulation was performed to investigate the flow pattern over a vertical drop featuring a sudden contraction under various contraction ratios. The simulation employed the RNG k-ε turbulence model in conjunction with the volume of fluid (VOF) method to capture free surface dynamics. The computational model was validated against experimental data, yielding acceptable levels of accuracy based on average percentage error (APE) and root mean square error (RMSE) metrics. Moreover, results indicate that a reduction in the contraction ratio leads to an increase in the falling jet thickness and hydraulic jump height, accompanied by a decrease in the water jet length. These changes promote enhanced energy dissipation, which is critical for reducing the kinetic energy of the flow in hydraulic structures such as irrigation canals, wastewater collection systems, and spillways. The findings suggest that optimizing the contraction ratio is an effective design parameter for improving energy dissipation efficiency and overall hydraulic performance.

1. Introduction

Vertical drops are employed when the natural ground slope exceeds the permissible channel slope. These structures are widely utilized in irrigation canals, wastewater collection systems, surface water distribution networks, and stepped spillways to dissipate kinetic energy while enhancing aeration and increasing dissolved oxygen levels. In such systems, the kinetic energy of the flow is predominantly dissipated as the falling water jet entrains ambient air. In general, there are two main approaches for research in this field: experimental investigations and numerical simulations. In recent years, the use of numerical simulations has become increasingly prevalent due to its cost-effectiveness and the ability to obtain more detailed insights into the subject under investigation. Historically, numerical simulations have been employed across a wide range of disciplines (Kohzadi, Mohammadi and Eghbalzadeh, 2024; Ajeel Fenjan, Akhtari and Gholami, 2022; Razmi, Saneie and Basirat, 2022).

Various experimental, theoretical, and analytical research on hydraulic behaviors of flow over drops were carried out by different researchers. Bakhmeteff (1932) was the first to study the hydraulic

*Corresponding author Email: afeghbal@razi.ac.ir

parameters of vertical drops. Moore (1943) presented a relationship for hydraulic parameters of vertical drops using experimental results. He stated that a part of the flow energy loss occurred due to the impact of the jet on the downstream channel.

In addition, Rand (1955), using his experimental results and former research, especially those of Moore (1943), presented a relationship for important drop parameters. Gill (1979) later demonstrated through experimental investigation that energy dissipation arises primarily from the collision of the jet with the downstream vortex. Hager (1983) examined the flow depth at the drop edge and formulated expressions for both the jet profile and the upstream water surface.

In addition, Chanson (1994) introduced semi-empirical relationships for assessing flow characteristics by combining streamline equations with the equation of momentum. Based on experimental data and the assumption that significant energy loss occurs at the junction between water jets and the downstream pool. Rajaratnam and Chamani (1995) developed a method for computing the hydraulic characteristics of the vortex. Rajaratnam and Wu (1998) further explored the influence of downstream flow depth on the overall flow pattern. Furthermore, Chamani and Beirami (2002) and Chamani, Rajaratnam and Beirami (2008) measured energy dissipation, downstream water depth, and vortex depth under different Froude number conditions and proposed methods to estimate energy loss using the similarity between surface turbulent shallow jet and the flow on a drop. Ming Hong, Shin Huang and Wan (2010) conducted experiments under supercritical flow conditions and developed semi-empirical regression relationships for predicting the vertical drop force and the length of the falling jet.

In recent years, numerical simulation has emerged as a powerful tool for investigating complex flow patterns. This approach offers advantages over experimental methods, including lower costs and the ability to capture detailed flow field characteristics (Versteeg and Malalsekera, 2007). Mansouri and Ziaee (2011) performed two-dimensional simulations of vertical drops using a commercial software. Fereshtepour et al. (2012) examined the hydraulic parameters of drops with both convergent and divergent transitions using OpenFOAM. Janfeshan Araqi and Lashkar Bolook (2003) investigated the effects of drop height and hydraulic characteristics on the flow over a drop with FLOW-3D software, and Tsai, Yen and Lin (2014) numerically studied the impact of downstream pool height located at the downstream of the drop on flow pattern and energy loss.

While previous studies have explored the hydraulic behavior of vertical drops using experimental and numerical methods, most investigations have focused on conventional configurations without explicitly addressing the influence of upstream channel contraction ratios on flow characteristics. Notably, existing literature lacks an analysis of how varying contraction ratios affect the flow dynamics, energy dissipation, and free surface profiles over vertical drops. Therefore, the primary objective of this study was to investigate the effects of different contraction ratios on the flow field characteristics, including falling jet thickness, hydraulic jump height, water jet length, and energy dissipation, over vertical drops with sudden contractions. This was achieved through three-dimensional numerical simulations employing the RNG k-ε turbulence model and the Volume of Fluid (VOF) method.

2. Materials and methods
2.1. Governing equations

The governing equations for incompressible turbulent flow consist of the continuity and Navier–Stokes equations (Eqs. 1 and 2) (Othman Ahmed et. al., 2021):

$$\frac{\partial U_i}{\partial x_i} = 0.0 \tag{1}$$

$$\frac{\partial U_i}{\partial t} + U_j \frac{\partial U_i}{\partial x_j} = \frac{1}{\rho} \frac{\partial}{\partial x_j}\left[-P\delta_{ij} + \rho v_t(\frac{\partial U_i}{\partial x_j} + \frac{\partial U_j}{\partial x_i}) \right] \tag{2}$$

where U_i and U_j denote the velocity components, x_i and x_j (i,j=1,2,3) represent the Cartesian coordinates, t is time, ρ is the fluid density, P is the pressure, δ_{ij} (i,j=1,2,3) is the Kronecker delta, and v_t is the turbulent eddy viscosity.

The free surface was modeled using the volume of fluid (VOF) method. The advection equation for calculating the volume fraction F of the fluid is given by Eq. 3.:

$$\frac{\partial F}{\partial t} + u\frac{\partial F}{\partial x} + v\frac{\partial F}{\partial y} + w\frac{\partial F}{\partial z} = 0 \tag{3}$$

A cell is considered completely filled with water when F=1 and entirely filled with air when F=0. Air areas are those in which there is no fluid mass, and a monotonous pressure is dominant (Hirt and Nichols, 1981). It should also be noted that the free surface was determined where F=0.5.

In the present work, the RNG k-ε turbulence model was employed to capture the complex turbulent flow dynamics in the vertical drop configuration. This model is utilized to simulate regions of high shear and turbulence with enhanced accuracy compared to the standard k–ε model (Sicilian and Harper, 1987).

The RNG k-ε framework solves two equations for turbulent kinetic energy (k) and its dissipation rate (ε) given by Eqs. 4 and 5:

$$\frac{\partial(\rho k)}{\partial t} + \frac{\partial(\rho u_i k)}{\partial x_i} = \frac{\partial}{\partial x_j}\left(\alpha_k \mu_{eff} \frac{\partial k}{\partial x_j} \right) + G_k - \rho\varepsilon \tag{4}$$

$$\frac{\partial(\rho\varepsilon)}{\partial t} + \frac{\partial(\rho u_i \varepsilon)}{\partial x_i} = \frac{\partial}{\partial x_j}\left(\alpha_\varepsilon \mu_{eff} \frac{\partial \varepsilon}{\partial x_j} \right) + C_{1\varepsilon}\frac{\varepsilon}{k}G_k - C_{2\varepsilon}\rho\frac{\varepsilon^2}{k} - R_\varepsilon \tag{5}$$

Here α_k and α_ε denote the inverse effective Prandtl number for k and ε, respectively. $C_{1\varepsilon}$ and $C_{2\varepsilon}$ are the model constants ($\alpha_k = 1.39, \alpha_\varepsilon = 1.39, C_{1\varepsilon} = 1.42,$ and $C_{2\varepsilon} = 1.68$). The effective viscosity, μ_{eff}, is expressed as the sum of molecular, μ, and turbulent, μ_t, viscosities ($\mu_{eff} = \mu + \mu_t$), where $\mu_t = \rho C_\mu \frac{k^2}{\varepsilon}$ ($C_\mu = 0.0845$).

The kinetic energy production term, G_k, and the additional term, R_ε, are computed as Eqs. 6 and 7:

$$G_k = \mu_t \left(\frac{\partial u_i}{\partial x_j} + \frac{\partial u_j}{\partial x_i} \right) \frac{\partial u_i}{\partial x_j} \tag{6}$$

$$R_\varepsilon = \frac{C_\mu \rho \eta^3 \left(1 - \frac{\eta}{\eta_o}\right)}{(1 + \beta\eta^3)} \frac{\varepsilon^2}{k} \tag{7}$$

where, η is the turbulence-to-strain rate ratio ($\eta = \frac{k}{\varepsilon}\sqrt{2S_{ij}S_{ij}}$). S_{ij} is the mean strain rate tensor, $S_{ij} = \frac{1}{2}\left(\frac{\partial u_i}{\partial x_j} + \frac{\partial u_j}{\partial x_i}\right)$. $\eta_o = 4.38$ and $\beta = 0.012$ are empirical constants.

2.2. Numerical model setup

Three-dimensional numerical simulations were conducted to investigate the flow field characteristics over vertical drops with sudden contractions under varying contraction ratios (b/B = 0.6, 0.7, 0.8, and 0.9). The contraction ratio (b/B) represents the ratio of the contraction width (b) to the upstream channel width (B). To validate the numerical model, experimental data from Jannati (2009) were used. Jannati's experiments were conducted in a horizontal flume with a length of 8.0 m, a height of 0.42 m, and a width of 0.40 m with a rough bed in the upstream channel. A sudden rectangular contraction with a thickness of 1 cm and a contraction ratio b/B=0.9 was located 4 m from the inlet. The plan view and overall configuration of the drop are shown in Fig. 1.

As depicted in Fig. 1a, Y, Y_0, Y_p and Y_1 are the initial flow depth, water height at the drop edge, the depth of the return flow and depth of the water after the hydraulic jump, respectively. The lengths of the drop and the water jet are denoted by L_d and L_{wj}, respectively.

Jannati (2009) specified an inlet discharge of Q=0.028 m³/s and an inlet flow depth of 95 mm.

The computational domain was designed to replicate the experimental flume geometry. A non-uniform grid with refined cells near the drop was employed to accurately capture the complex flow features. The non-uniform grid consisted of 400, 68, and 50 cells in the x, y and z directions, respectively, with the first cell positioned such that the dimensionless parameter, y+, defined by Eq. 8. exceeded 30 (Versteeg and Malalsekera, 2007):

$$y^+ = \frac{y_f u_*}{v} \tag{8}$$

where, y_f is the distance of the first node from the wall, u_* is the shear velocity and v is the kinematic viscosity.

Two criteria of the root mean square error, RMSE (Eq.9.), and the average percentage error, APE (Eq.10.), were applied to evaluate the accuracy of the numerical simulation results (Othman Ahmed et. al., 2024).

$$RMSE = \sqrt{\frac{1}{n}\sum_{i=1}^{N}\left(R_{(Exp)} - R_{(Num)}\right)^2} \tag{9}$$

$$APE = \frac{100}{N} \sum_{i=1}^{N} \left| \frac{R_{(Exp)} - R_{(Num)}}{R_{(Num)}} \right| \qquad (10)$$

where, $R_{(Exp)}$ and $R_{(Num)}$ are the experimental and numerical results, respectively.
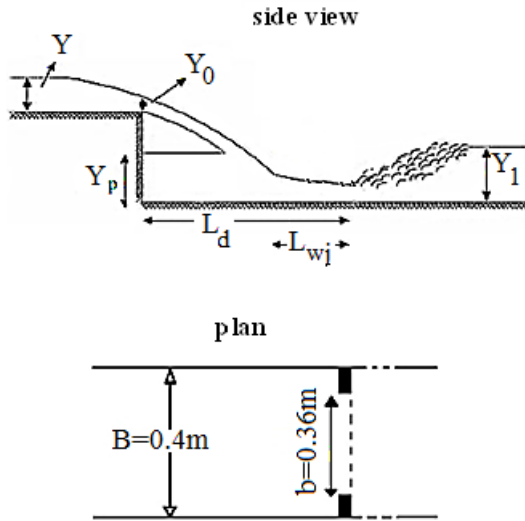

Fig. 1. General view of the vertical drop structure with a convergent transition.

3. Results and discussion

As mentioned earlier, the numerical simulation results were verified against the experimental measurements conducted by Jannati (2009).

Fig. 2 presents a comparison of non-dimensional longitudinal velocity profiles between numerical simulations and experimental data. This comparison focuses on three transverse positions (z = 0.1 m, 0.2 m, and 0.3 m) located 1.65 cm downstream of the drop edge. In Fig. 2, the horizontal and vertical coordinates are non-dimensionalized using the inlet velocity, u_1, and the vertical drop height, h, respectively. As this figure shows, there is an acceptable agreement between the numerical simulation and experimental results. The simulation closely matches the experimental data at the central transverse position (z = 0.2 m), with minimal deviations across the entire vertical profile. This indicates that the numerical model effectively captures the core flow dynamics in regions away from the sidewalls.

Near the side walls (z = 0.1 and 0.3 m), the simulated and experimental profiles diverge, particularly near the free surface. These discrepancies align with the reported APE of 6.92% and 6.86% for

these positions, respectively. The deviations may be attributed to wave effects at the free surface, which are challenging to model precisely due to unsteady air-water interactions. Flow dispersion toward the sidewalls, causing secondary currents and boundary layer effects not fully captured by the turbulence model.

Both simulation and experiment show a velocity peak near the drop edge (lower y/h), indicating accelerated flow as water transitions over the vertical drop. The velocity decreases toward the channel bed, consistent with boundary layer effects.

Table 1 presents the RMSE and APE values for the longitudinal velocity at the three transverse positions z= 0.1, 0.2, and 0.3m. As this table presents, the highest errors were observed at z=0.1 and 0.3 m, attributable to wave effects downstream of the falling jet and flow dispersion toward the side walls, while the lowest error occurred at z=0.2 m.

Table 1. The RMSE and APE values of the simulated velocities

z (m)	RMSE	APE, %
0.1	0.17	6.92
0.2	0.07	2.73
0.3	0.19	6.86

Additionally, the water height at the drop edge was measured as 0.075 m in the experiments of Jannati (2009), whereas the simulation predicted a value of 0.070 m. The RMSE and APE for the water height were 0.005 m and 6.6%, respectively, demonstrating that the numerical model accurately simulates the flow pattern over the vertical drop with a convergent transition.

Subsequent analyses were performed using four different contraction ratios (b/B=0.9,0.8,0.7, and 0.6) to evaluate their effects on flow characteristics.

Fig. 3 presents streamline patterns for two representative contraction ratios: a) b/B = 0.8 and b) b/B = 0.6.

The free surface profile along the central axis, extending from the drop edge (x=0) to x=1.6 m downstream, was also examined. The vertical drop creates a sudden narrowing, leading to complex flow dynamics, including vortices, jet formation, and hydraulic jumps. A decrease in the contraction ratio was found to increase the falling jet thickness, while the water height immediately downstream of the falling jet decreased and the hydraulic jump height increased.

Fig. 4 illustrates the transverse free surface profiles in the downstream channel for different contraction ratios, evaluated at two locations: x = 0.15 m (near the drop edge), and x = 0.6 m (downstream of the falling jet). At x=0.15 m, a reduction in the contraction ratio from 0.9 to 0.8 resulted in a decrease in flow depth; however, further reductions in the contraction ratio led to an increase in central flow depth, likely due to intensified turbulence and vortices (Fig. 4a). The free surface becomes more uneven, with deeper flow near the sidewalls at lower contraction ratios (b/B ≤ 0.7).
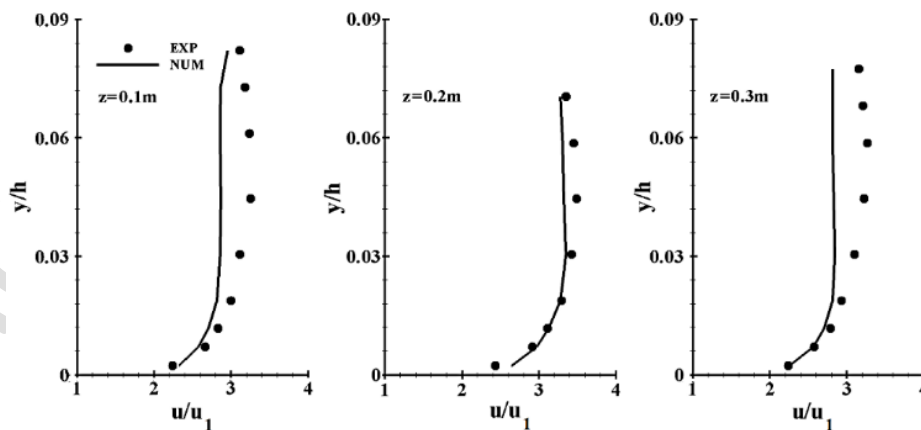

Fig. 2. Comparison of simulated non-dimensional longitudinal velocity in the section 1.65 cm downstream the drop edge at three transverse positions z=0.1, 0.2, 0.3 m with the experimental results reported by Jannati (2009).
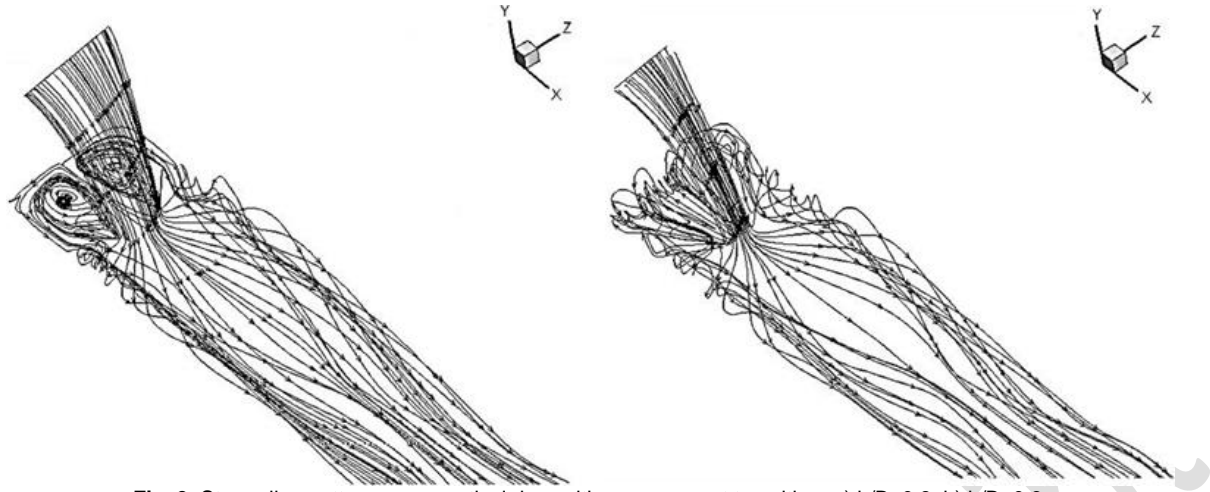
Fig. 3. Streamline patterns over vertical drop with a convergent transition: a) b/B=0.8; b) b/B=0.6.
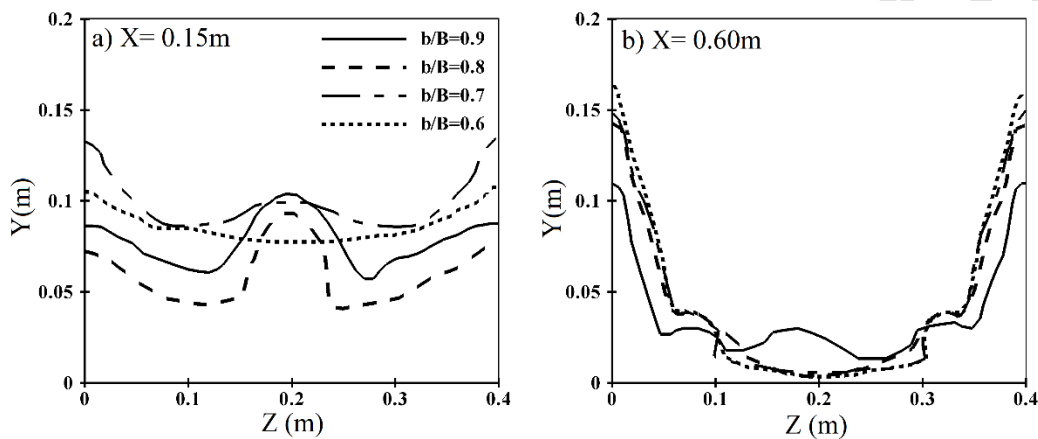

Fig. 4. Transverse free surface profiles in the downstream channel for different contraction ratios.

At x=0.6 m, decreasing the contraction ratio caused a reduction in the central flow depth and an increase in the flow depth near the side walls, consistent with the formation of recirculation zones and turbulent mixing. (Fig. 4b). Fig. 4 quantitatively demonstrates that contraction ratios directly govern lateral flow redistribution. For instance, at x = 0.6 m, the flow depth gradient between the centerline and sidewalls increases as b/B decreases, indicating stronger secondary currents.

Beyond the hydraulic jump (at x=1.6 m), the free surface became relatively uniform, with minimal variations near the side walls. Furthermore, a decrease in the contraction ratio resulted in a narrower falling jet and an increased water height at the drop edge.

Fig. 5 compares the water jet lengths, L_{wj}, along the central axis of the channel for different contraction ratios. This figure demonstrates a systematic decrease in L_{wj} as the contraction ratio reduces, highlighting the critical role of geometric constraints in jet dynamics. The data show a strong inverse correlation between b/B and L_{wj}. For example, at b/B = 0.6, the water jet length is approximately 30% shorter compared to the case b/B = 0.9.
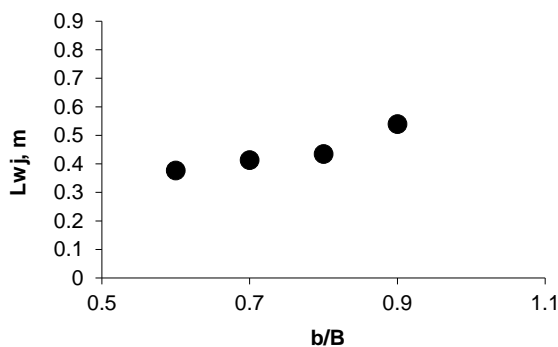
Fig. 6 presents the drop length, L_d, defined as the distance from the drop edge to the initiation point of the hydraulic jump, along two transverse sections z = 0.15 m, and z = 0.2 m for different contraction ratios. This illustration demonstrates a subtle yet systematic decrease in L_d as the contraction ratio reduces. This suggests that the contraction ratio has little influence on the initiation point of the hydraulic jump along the central axis.

A reduction in b/B leads to a gradual shortening of L_d (e.g., L_d decreases approximately 12% from b/B = 0.9 to 0.6 at both transverse sections). This trend aligns with the study's findings that lower contraction ratios accelerate flow and enhance turbulence, promoting earlier hydraulic jump formation.
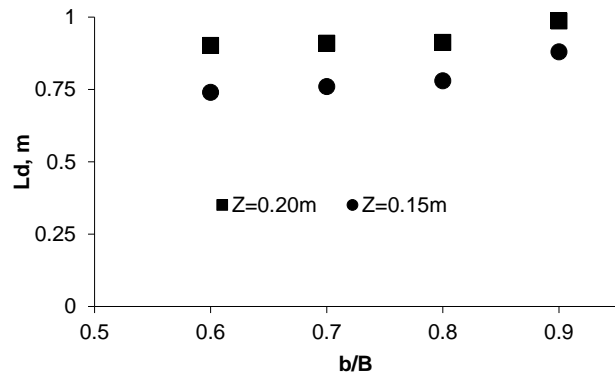

Fig. 6. The drop length for different contraction ratios in two transverse sections.

Fig. 5. The water jet length for different contraction ratios.

The longitudinal velocity profiles upstream of the hydraulic jump along the central axis of the channel at x=0.6 m (downstream of the falling jet) for two transverse positions z = 0.1 m, and z = 0.2 m are shown in Fig. 7 for different contraction ratios. A reduction in the contraction ratio from 0.9 to 0.7 led to a decrease in velocity near the side walls, whereas a further reduction to 0.6 produced an increase in

the longitudinal velocity (Fig. 7a). Along the central axis, the velocity increased as the contraction ratio decreased (Fig. 7b).

Overall, the decrease in the contraction ratio resulted in higher relative energy losses. In vertical drops, energy loss is primarily attributed to the formation of rotational flow upstream of the falling jet

and the development of a hydraulic jump downstream. Therefore, the present study demonstrates that reducing the contraction ratio not only alters the flow field characteristics but also significantly enhances energy dissipation.
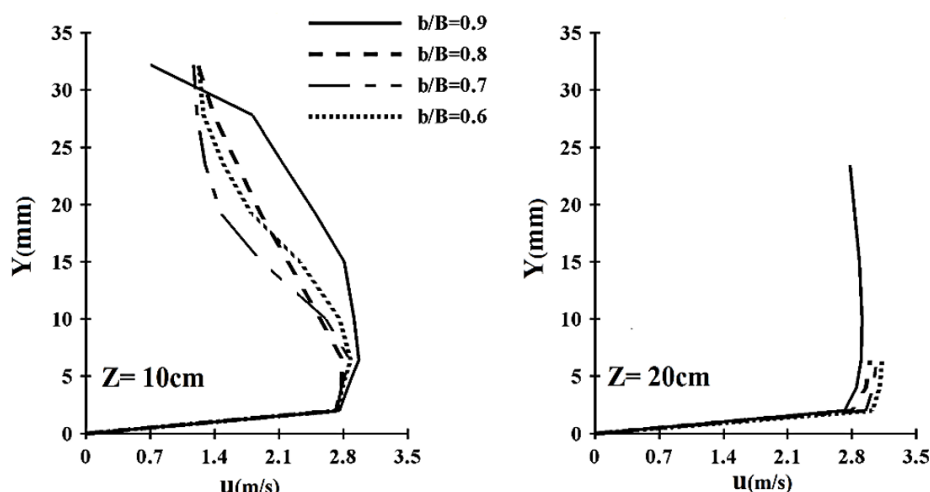

Fig. 7. The longitudinal velocity profiles at upstream of the hydraulic jump in the central axis at x=0.6 in different points z= 0.1 and 0.2 m.

4. Conclusions

This study conducted three-dimensional numerical simulations of vertical drops with sudden convergent transitions using commercial software that incorporated the RNG k–ε turbulence model and the volume of fluid (VOF) method. Validation against experimental data confirmed that the numerical model effectively reproduces the complex flow patterns over the drop, as evidenced by low APE and RMSE values. The results indicate that decreasing the contraction ratio increases the falling jet thickness, relative energy loss, and hydraulic jump height, while reducing the water jet length. These insights underscore the importance of considering upstream channel geometry in the design and optimization of energy dissipation facilities. Future research may extend these findings by incorporating additional factors such as variable flow rates, different turbulence models, and three-dimensional effects in more complex geometries.

Nomenclature

APE	Average percentage error
b/B	Contraction ratio
F	Volume fraction of fluid
Ld	Drop length
Lw	Water jet length
P	Pressure
Q	Flow discharge
RMSE	Root mean square error
T	Time
Ui, Uj	Velocity components
VOF	Volume of fluid method
xi, xj	Cartesian coordinates
y+	Dimensionless wall distance
Y	Initial flow depth
Y0	Water height at the drop edge
Yp	Depth of the return flow
Y1	Depth of the water after hydraulic jump

Author Contributions

Hossein Shahin: Writing, investigation, software, analyzing the results and conclusion
Afshin Eghbalzadeh: Supervisor, writing, review and control of results, analyzing the results and conclusion
Mitra Javan: Co-advisor, research design, analyzing the results and conclusion

Conflict of Interest

The authors declare that they have no conflict of interests.

Acknowledgement

Data Availability Statement

Data will be made available on reasonable request.

References

Ajeel Fenjan, S., Akhtari, A.A. and Gholami, A. (2022) 'Determination of discharge coefficient in the tilted crown sharp-crested weirs', *Journal of Applied Research in Water and Wastewater*, 9(2), pp. 180–186. doi: https://doi.org/10.22126/arww.2022.2538.1216

Bakhmeteff, B. (1932) Hydraulics of open channels. 1th edn. New York: McGraw-Hill.

Chamani, M.R. and Beirami, M.K. (2002) 'Flow characteristic at drops', *Journal of Hydraulic Engineering*, 128(8), pp. 788–791. doi: https://doi.org/10.1061/(ASCE)0733-9429(2002)128:8(788)

Chamani, M.R., Rajaratnam, N. and Beirami, M.K. (2008) 'Turbulent jet energy dissipation at vertical drops', *Journal of Hydraulic Engineering*, 134(10), pp. 1532–1535. doi: https://doi.org/10.1061/(ASCE)0733-9429(2008)134:10(1532)

Chanson, H. (1994) 'Comparison of energy dissipation between nappe and skimming flow regimes on stepped chutes', *Journal of Hydraulic Research*, 32(2), pp. 213–218. doi: https://doi.org/10.1016/0022-1694(94)90024-3

Fereshtepour, M. *et al.* (2012) 'Three-dimensional simulation of the flow over vertical drop with convergent and divergent transitions using OpenFOAM software', *Proceedings of the 11th Iranian Hydraulic Conference*. Urmia, Iran, 6-8 Nov. Urmia: University of Urmia, pp. 1-7.

Gill, M.A. (1979) 'Hydraulics of rectangular vertical drop structures', *Journal of Hydraulic Research*, 17(4), pp. 289–302. doi: https://doi.org/10.1016/0022-1694(79)90010-8

Hager, W.H. (1983) 'Hydraulic stresses on an overfall', *Journal of Hydraulic Engineering*, 109(12), pp. 1683–1697. doi: https://doi.org/10.1061/(ASCE)0733-9429(1983)109:12(1683)

Hirt, C. and Nichols, B. (1981) 'Volume of fluid (VOF) method for the dynamics of free boundaries', *Journal of Computational Physics*, 39, pp. 201–225. doi: https://doi.org/10.1016/0021-9991(81)90052-4

Janfeshan Araqi, H. and Lashkar Bolook, H. (2013) 'Presenting a criterion for predicting the flow pattern over a vertical drop based on its hydraulic and geometric characteristics', *Proceedings of the 12th Iranian Hydraulic Conference*. Tehran, Iran, 29-31 Oct. Tehran: University of Tehran, pp.1-8.

Jannati, H. (2009) Vertical drop with a contraction transition and subcritical flow upstream. MS Dissertation. Isfahan University of Technology.

Kohzadi, A., Mohammadi, K. and Eghbalzadeh, A. (2024) 'Application of various methods in design for control of bed erosion and river modification aiding numerical simulation', *Journal of Applied Research in Water and Wastewater*, 11(2), pp. 151–161. doi: https://doi.org/10.22126/arww.2025.10877.1338

Mansouri, R. and Ziaee, A.N. (2011) 'Two-dimensional numerical simulation of flow pattern in vertical drop considering different boundary situations', *Proceedings of the 6th National Congress on Civil Engineering*. Semnan, Iran, 26-27 Apr. Semnan: Semnan University, pp. 1-7.

Ming Hong, Y., Shin Huang, H. and Wan, S. (2010) 'Drop characteristics of free-falling nappe for aerated straight-drop spillway', *Journal of Hydraulic Research*, 48(1), pp. 125–129. doi: https://doi.org/10.1016/j.jhydro.2009.12.001

Moore, W.L. (1943) 'Energy loss at the base of free overfall', *Transactions of the American Society of Civil Engineers*, 108, pp. 1343–1360. doi: https://doi.org/10.1061/(ASCE)0733-9429(1943)108:1343

Othman Ahmed, K. *et al.* (2021) 'Numerical modeling of depth and location of scour at culvert outlets under unsteady flow conditions', *Journal of Pipeline Systems Engineering and Practice*, 12(4), p. 4021040. doi: https://doi.org/10.1061/(ASCE)PS.1949-1204.0000578

Othman Ahmed, K. *et al.* (2024) 'Numerical modelling of downstream scour in circular culverts: Impact of inlet blockages and variable flow conditions', *Plos One*, pp. 1–25. doi: https://doi.org/10.1371/journal.pone.0312501

Rajaratnam, N. and Chamani, M.R. (1995) 'Energy loss at drops', *Journal of Hydraulic Research*, 33(3), pp. 373–384. doi: https://doi.org/10.1061/(ASCE)0733-9429(1995)33:3(373)

Rajaratnam, N. and Wu, S. (1998) 'Impinging jet and surface flow regimes at drops', *Journal of Hydraulic Research*, 36(1), pp. 69–74. doi: https://doi.org/10.1061/(ASCE)0733-9429(1998)36:1(69)

Rand, W. (1955) 'Flow geometry at straight drop spillways', *Proceedings of the American Society of Civil Engineers*, 81, pp. 1–13. doi: https://doi.org/10.1061/(ASCE)0733-9429(1955)81:1(1)

Razmi, M., Saneie, M. and Basirat, S. (2022) 'Comparative evaluation of CFD model and intelligence hybrid method to ameliorate ANFIS in side weir coefficient of discharge modelling', *Journal of Applied Research in Water and Wastewater*, 9(2), pp. 125–140. doi: https://doi.org/10.22126/arww.2023.7934.1255

Sicilian, J.M., Hirt, C.W. and Harper, R.P. (1987) FLOW-3D. Computational Modeling Power for Scientists and Engineers. Report FSI-87-00-1. Flow Science, Los Alamos.

Tsai, C.P., Yen, C.C. and Lin, C. (2014) 'Simulations on skimming flow over a vertical drop pool', *Journal of Engineering Mechanics*, 140(7), 04014044. doi: https://doi.org/10.1061/(ASCE)0733-9429(2014)140:7(04014044)

Versteeg, H.K. and Malalasekera, W. (2007) An introduction to computational fluid dynamics: The finite volume method. 2nd edn. London: Pearson Education.